Numerical Analysis on Vibro-acoustic Characterisation of Hybrid Honeycomb Structure with Flow Permeability

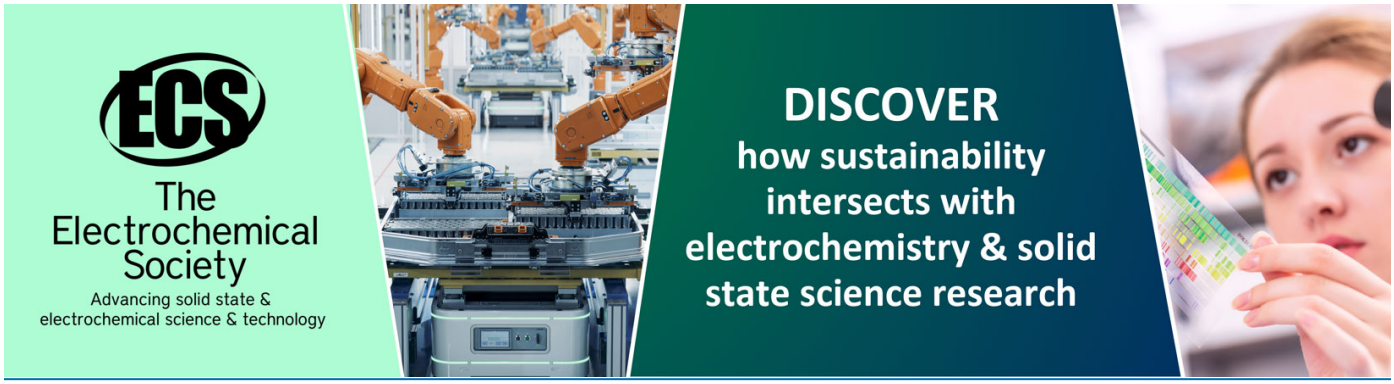

Numerical Analysis on Vibro-acoustic Characterisation of Hybrid Honeycomb Structure with Flow Permeability

Zhen Wei Tee and Choe Yung Teoh*

Faculty of Engineering and Technology, Tunku Abdul Rahman University College, Kuala Lumpur, Malaysia
*Corresponding author: teohcy@tarc.edu.my

Abstract. The application of conventional noise attenuating structures was often limited when the exchange of air was required due to the trade-off between their noise attenuation properties and ventilation efficiency. The large physical footprint of conventional noise attenuating structures with flow permeability had also limited their applications. This paper investigated the use of corrugation structure in lightweight honeycomb sandwich panels with flow permeability to improve noise attenuation while preserving ventilation. The vibro-acoustic property of the honeycomb structure with flow permeability at low to medium frequency range (50-3000 Hz) was investigated through numerical simulation. Two different hybrid panel designs with U-shaped and V-shaped corrugations in the honeycomb core had been proposed and were found to exhibit superior sound transmission loss (STL) compared to the honeycomb panel without significantly affecting the flow performance. It was found that in the frequency range of 50-3000 Hz, the unweighted STL of the U-shaped corrugation honeycomb hybrid panel (UCHP) and V-shaped corrugation honeycomb hybrid panel (VCHP) was 19 dB and 25 dB higher than the honeycomb panel respectively with negligible effect on the flow performance. The proposed hybrid panel showed promising noise attenuation applications which involved fluid flows such as in fan and engine noise reduction.

1. Introduction

Noise control measures such as using sound isolators, sound absorbers, mufflers, baffles, as well as redesigning of sound sources were often used to reduce the excessive noise as well as their adverse impact on the human and environment. These conventional noise attenuation material and structures such as high-density panels and micro-perforated panel (MPP) with rigid backing relied on sound reflection or sound absorption to prevent the transmission of sound across a boundary. However, these sound attenuation materials or structures often stopped both the acoustic wave transmission and steady fluid flow across the boundary which eliminated the passage of air. As a result, this limited their applications when the exchange of air was necessary or advantageous such as in noise control of cooling fans where free circulation of air was important in order to allow heat transfer and dissipation. Besides, noise reduction in the low frequency region (<500 Hz) using conventional approaches was challenging and often involved increasing the thickness of acoustic barrier layer as the transmission of noise through a material was inversely proportional to the product of the frequency, material density and material thickness [1].

To date, several approaches and acoustic enclosure with openings had been proposed or designed to block sound while maintaining the transport of air. For instance, diffraction type resonator with negative effective bulk modulus was utilized in designing a soundproof window that was transparent to airflow [2]. The use of an acoustic metamaterial with a large orifice to allow airflow while

achieving narrow-band sound insulation through the interaction of resonating field of four membranes had also been demonstrated [3]. Several studies had also applied active noise control to simultaneously achieve acoustic insulation and natural ventilation [4, 5]. Although the transmission loss or sound absorption properties of the mentioned designs were high, the structures generally had a large physical footprint or require the use of complex software and hardware which limited their application for real-world problems such as reducing noise from fans and compressors [6].

Among various lightweight structure, honeycomb panel was one of the most commonly used structure in the industries with wide application due to its high strength to weight ratio. Although the characterisation of the honeycomb structure had been subjected to many scientific works from the mechanical viewpoint, research on the acoustic characteristics of honeycomb structure was still lacking, especially in the area involving the transfer of fluid. Several studies had also demonstrated that the honeycomb structure had promising potential in achieving noise attenuation while allowing for the transfer of air [6, 7]. Besides, hybrid-cored sandwich panels had also been shown to possess superior mechanical strength and impact energy absorption ability which could improve the stiffness of the panel as well as its acoustic properties [8, 9].

This paper investigated the use of hybrid honeycomb structure to achieve noise attenuation while maintaining air permeability. The vibro-acoustic properties of the honeycomb panel at low to medium frequency range (50-3000 Hz), as well as its flow performance, was studied and analysed through numerical simulations with commercial ANSYS software. The improvement on sound attenuation properties via the use of corrugation structure to form the hybrid honeycomb structure was then investigated.

2. Methodology

Numerical analysis with finite element method (FEM) was conducted to investigate the vibro-acoustic performance of the honeycomb panel design with flow permeability. Numerical method was used as it allowed the study of complex structure or situation that would otherwise be too time-consuming or difficult to be solved analytically. Besides, with finite element method, the bi-directional coupling of the fluid-structure interaction between a structural body and a fluid such as air could be taken into account in the acoustic analysis.

2.1. Honeycomb panel design

A honeycomb panel (HP) which consisted of two faceplates with the honeycomb cores in between as shown in figure 1, was developed and used as the baseline for the numerical analysis. The dimension of the honeycomb panel was summarized in table 1 and the geometric structure of the honeycomb cell was illustrated in figure 2. To allow for air permeability, both the top and bottom facings of the honeycomb panel were perforated with macro-sized holes of 10 mm. The perforated holes were located concentrically with the honeycomb core so that air would be allowed to flow through the honeycomb cavity before passing through the panel via the perforated hole at the bottom faceplate as shown in figure 3. The open area ratio of the honeycomb panel developed was also computed as 14.1% using equation (1):

$$\mathrm{OAR} = \frac{A_{open}}{A_{total}} \text{ x } 100\% \tag{1}$$

where A_{open} and A_{total} was the open area and total area of the honeycomb panel respectively.

Acrylonitrile butadiene styrene (ABS) plastic was selected as the material for the honeycomb panel to be used in the numerical analysis due to its low density. Besides, as ABS was a common material in 3D printing, the honeycomb panel could be fabricated easily through 3D printing for experimental validation of the simulation results in the future study.

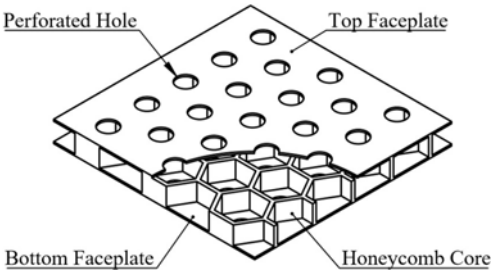

Figure 1. Schematic diagram of honeycomb sandwich panel with flow permeability

Table 1. Dimension of honeycomb panel

Dimension	Value
Faceplate Length, L_f	114.32 mm
Faceplate Width, W_f	112.00 mm
Faceplate Thickness, t_f	1.00 mm
Diameter of perforated hole, d	10.00 mm
Honeycomb cell size, H	20.00 mm
Thickness of honeycomb cell wall, b	2.00 mm
Thickness of honeycomb core, t_c	10.00 mm
Internal angle of honeycomb cell, θ	60°

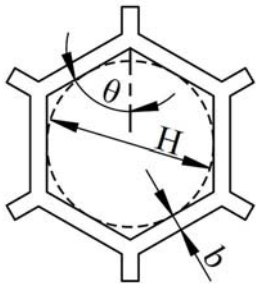

Figure 2. Geometric structure of honeycomb cell.

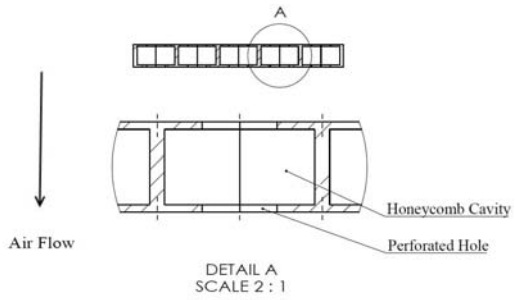

Figure 3. Detail view of perforated hole and honeycomb cavity.

2.2. Vibro-acoustic simulation model

The vibro-acoustic numerical simulation was conducted using ANSYS Harmonica Acoustic solver to calculate the acoustic response of a system due to excitation by a sinusoidal varying acoustic pressure where the excitation was continuous at a constant frequency. The acoustic simulation was conducted over a frequency range of 50-3000 Hz in order to determine the sound transmission loss (STL) of the honeycomb panel at low to medium frequency range. The fluid and material properties used for the numerical simulation were also summarised in table 2.

The simulation model consisted of an infinite duct that was divided by the honeycomb panel with perforated facing as shown in figure 4. Numerical analysis of a panel in a duct was used in this study

Table 2. Properties of fluid and material used for numerical analysis

Description	Symbol	Value	Unit
Fluid: Air			
Speed of sound	c_0	346.25	m/s
Density	ρ_0	1.225	$\mathrm{kg/m^3}$
Viscosity	μ_0	1.7894×10^{-5}	kg/ms
Material: Acrylonitrile butadiene styrene (ABS)			
Density	ρ	1040	$\mathrm{kg/m^3}$
Young Modulus	E	2.390	GPa
Poisson Ratio	v	0.399	
Bulk Modulus	K	3.944	GPa
Shear Modulus	G	0.854	GPa
Tensile Yield Strength	σ_y	41.4	MPa
Tensile Ultimate Yield Strength	σ_u	44.3	MPa
Percent Elongation	ε_e	24.3	%
Tangent Modulus	K	68.3	MPa

as it could provide physical insight for the design of the STL of a panel system and was more manageable than the partitions between two large reverberation chambers [10]. The boundary conditions applied to the numerical model for acoustic simulation were also illustrated in figure 5.

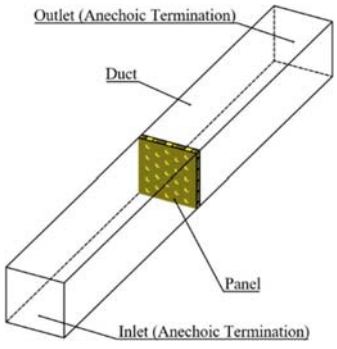

Figure 4. Simulation model for acoustic analysis.

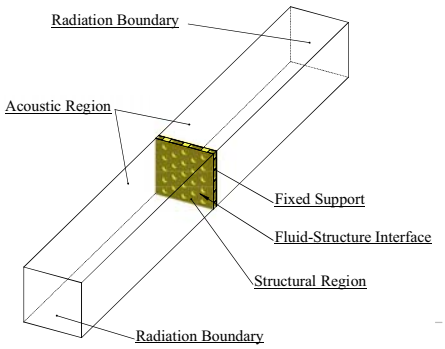

Figure 5. Boundary condition applied on numerical model.

As STL was source independent, a mass source, $\dot{M}$ with an arbitrary value of $1\ \mathrm{kg/m^2s}$ was applied on the upstream end face of the duct (inlet) as the acoustic excitation to generate the sound wave that would propagate along the duct until it stroke the honeycomb panel [11]. The sound would be transmitted through the honeycomb panel and propagated toward the downstream end face of the duct (outlet) where it was absorbed by the anechoic termination. With the constant mass source, $\dot{M}$ of $1\ \mathrm{kg/m^2s}$, the inlet sound pressure level, $\mathrm{SPL_{in}}$ was computed as 135.74 dB using equation (2):

$$\mathrm{SPL_{in}} = 20\log_{10}\left(\frac{p}{p_0}\right) - 20\log_{10}\left(\sqrt{2}\right) \quad (2)$$

where p_0 was the reference pressure of 20 μPa and p was the equivalent incident pressure for the mass source excitation which could be expressed as:

$$p = \frac{1}{2} Q p_0 c_0 \tag{3}$$

where Q was the acoustic source volume flow rate and c_0 was the speed of sound in air. The equivalent incident acoustic pressure, p and the sound pressure level, $\mathrm{SPL_{in}}$ were computed instead of measuring the average sound pressure level at the inlet face of the simulation model as the impedance change caused by the panel would cause the acoustic energy to be reflected back upstream toward the inlet. The reflection of acoustic energy would cause the sound pressure level measured at the inlet face to increase, hence resulting in an artificially higher STL if the measured incident acoustic sound pressure of the simulation model was used [12].

The outlet sound pressure level, $\mathrm{SPL_{out}}$ of the simulation was measured to compute the STL of the honeycomb panel which could be expressed by equation (5):

$$\mathrm{STL} = 20 \log_{10}\left(\frac{p_{\mathrm{incident}}}{p_{\mathrm{transmitted}}}\right) + 20 \log_{10}\left(\frac{S_{\mathrm{inlet}}}{S_{\mathrm{outlet}}}\right) \tag{4}$$

$$\mathrm{STL} = SPL_{\mathrm{in}} - SPL_{\mathrm{out}} + 20 \log_{10}\left(\frac{S_{\mathrm{inlet}}}{S_{\mathrm{outlet}}}\right) \tag{5}$$

where $p_{\mathrm{transmitted}}$ was the average pressure at the outlet face, S_{inlet} and S_{outlet} were the areas of the inlet and outlet face respectively. As the inlet and outlet faces of the duct were equal ($S_{\mathrm{inlet}} = S_{\mathrm{outlet}}$), equation (5) could be simplified as:

$$\mathrm{STL} = SPL_{\mathrm{in}} - SPL_{\mathrm{out}} \tag{6}$$

It should also be highlighted that plane wave conditions were assumed to exist at the inlet and outlet faces for equations (5) and (6) to be valid. The calculation of STL for non-plane wave condition would involve the use of real and imaginary part of the acoustic pressure and particle velocity, as well as the area at each node and at each frequency of the inlet and outlet faces to compute the acoustic intensity and effective nodal area in order to determine the sound power, and hence was not covered in this study [12].

The natural frequencies and mode shapes of the honeycomb panel with all lateral faces fixed were also extracted using ANSYS Modal solver. This was accomplished by solving the acoustic simulation model without the acoustic region and any excitation. The natural frequencies and mode shapes were extracted to investigate the acoustic performance of the panel at resonance.

2.3. Flow simulation model

As no mean flow could be included in the acoustic analysis due to a different formulation of wave equation was required if the mean flow was included, computational flow dynamics (CFD) simulation was conducted to analyse the flow performance of the honeycomb panel using ANSYS CFX solver. To simulate airflow in the duct, the acoustic excitation was replaced with airflow so that air would flow into the duct through the inlet and exit through the outlet after passing through the perforated facings and honeycomb cavity. The simulation was conducted at different inlet velocity, u ranging from $0.5\ \mathrm{m/s}$ to $3.0\ \mathrm{m/s}$ with a constant 5% turbulence to investigate the pressure loss at different inlet velocity. The pressure loss, ΔP due to the honeycomb panel was computed using equation (7):

$$\Delta P = P_{\mathrm{inlet}} - P_{\mathrm{outlet}} \tag{7}$$

where P_{inlet} and P_{outlet} was the inlet and outlet pressure respectively.

2.4. Hybrid honeycomb panel design

Two different hybrid honeycomb panel designs were proposed to improve the noise attenuation properties of the honeycomb panel without significantly impacting the flow performance. The improvements made were focus on the honeycomb core as the geometry and the dimension of the system would affect the sound insulation at low frequency [13, 14]. The improvements involved implementing corrugation structure in the honeycomb core to form a honeycomb-corrugation hybrid core. Two different corrugation structures which were U-shaped corrugation and V-shaped corrugation were proposed and investigated. Similar to the honeycomb panel design used in this study the corrugation structure was perforated such that it did not obstruct the airflow. In order to investigate the effect of the different corrugation structure in the honeycomb panel on the flow performance, the OAR of the two proposed panels was kept constant at 14.1%. The proposed U-shaped corrugation honeycomb hybrid panel (UCHP) and V-shaped corrugation honeycomb hybrid panel (VCHP) were illustrated in figure 6 and figure 7 respectively.

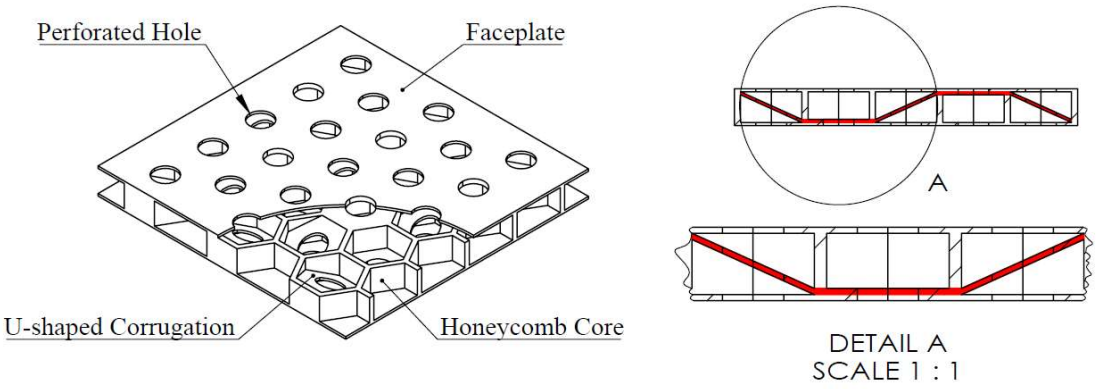

Figure 6. Schematic diagram of U-shaped corrugation honeycomb hybrid panel (UCHP)

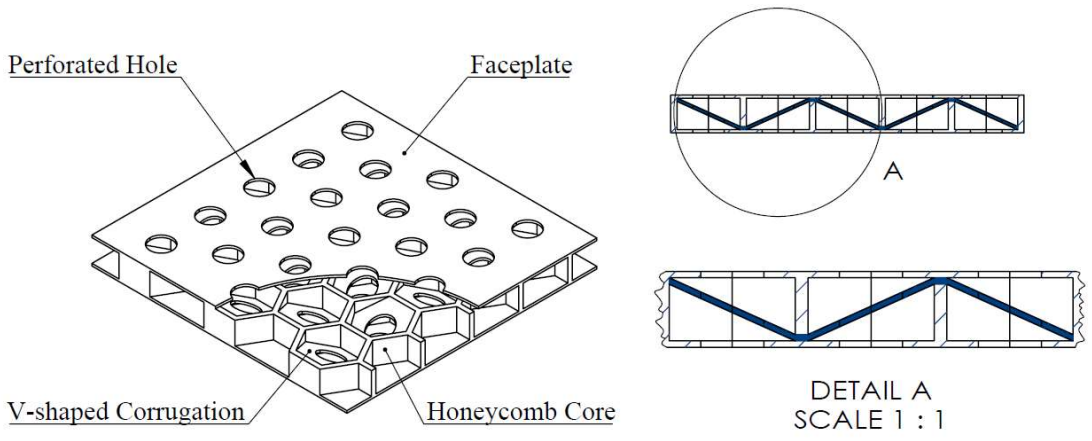

Figure 7. Schematic diagram of V-shaped corrugation honeycomb hybrid panel (VCHP)

3. Result and discussion

3.1. Modal analysis

From the modal analysis, the first six natural frequencies of the honeycomb panel (HP), UCHP and VCHP were computed and summarized in table 3. It could be observed that only the first natural frequency of the panels was located in the frequency range of 50-3000 Hz used in the acoustic simulation. This indicated that all three panels would undergo the first resonance in the acoustic simulation as their first natural frequency was located in the frequency range used in the acoustic simulation. Besides, it could be seen that at the same mode, the honeycomb panel had the highest natural frequency followed by UCHP and then VCHP, but the natural frequencies of the different panel designs were relatively close.

The mode shapes for the first natural frequency of the different panel designs were also illustrated in figure 8 and it could be seen that the UCHP and VCHP exhibited similar mode shapes with the honeycomb panel due to similar overall structure of the panels. It could also be observed that each of the panel exhibit flexural vibrations as the two faceplates bent in the same direction. Dilatational vibration which occurred when the faceplates bent in opposite direction and would result in undesirable coincidence response in the sound transmission spectrum of lightweight sandwich panels was not observed in the first six natural frequencies [15, 16].

Table 3. Natural frequencies of different panel designs

	Frequency (Hz)		
Mode	HP	UCHP	VCHP
1	1976.9	1901.2	1895.0
2	3342.6	3208.6	3186.0
3	3375.4	3344.4	3291.6
4	4449.4	4345.5	4306.0
5	4995.7	4818.0	4767.5
6	5063.4	4943.0	4944.1

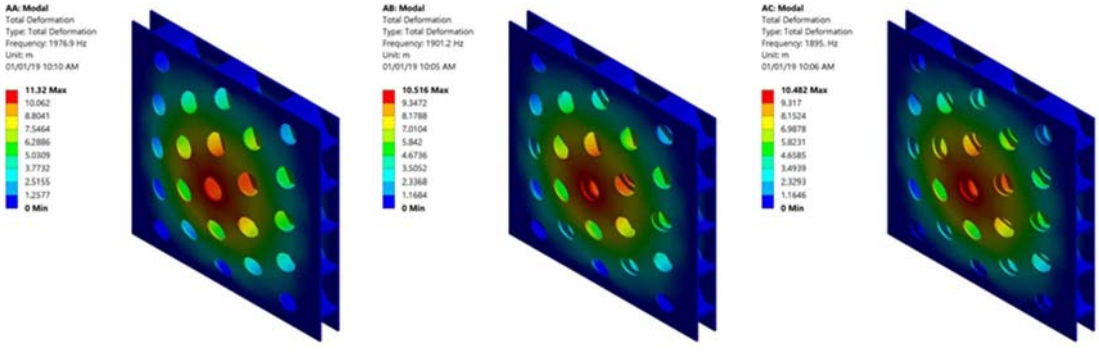

(a) HP (1976.9 Hz) (b) UCHP (1901.2 Hz) (c) VCHP (1895.0 Hz)

Figure 8. Mode shape of different panel designs at first natural frequency.

3.2. Vibro-acoustic performance

The average outlet sound pressure level, SPL_{out} was shown in figure 9 and it could be seen that the SPL_{out} for each panel design was always lower than the computed inlet sound pressure level, SPL_{in} of 135.74 dB, implying that the sound level was reduced after passing through the panel. The STL of different panel designs was also shown in figure 10 and it could be seen that in the low to medium frequency region, the STL decreased as the frequency increased. It was also observed that the STL of the VCHP was the highest, followed by the UCHP and the honeycomb panel. A rapid reduction in the STL was also observed from figure 10 near the first resonance frequency of the panel as the panel resonated with the acoustic excitation which caused a rapid reduction in sound insulation. A higher STL observed in the stiffness-controlled region which was located at the low frequency region before the first resonance frequency for UCHP and VCHP generally implied that the UCHP and VCHP had a higher stiffness compared to the honeycomb panel due to the presence of the corrugation structure which stiffness the panel and improved the STL [8, 9]. Although increasing the stiffness of the panel would generally lower the coincidence frequency in the coincidence region but it was not considered in the present study as the coincidence region was located at the higher frequency region and high frequency noise could be damped more easily using conventional noise attenuation method [17].

As the STL of the different panels varied with similar trends when the frequency increased, the unweighted average STL value for the frequency range of 50-3000 Hz was computed and tabulated in table 4. The unweighted average STL value was used to provide a single number rating of the transmission loss to evaluate the acoustic performance of the panel. It could be seen that the VCHP had the highest unweighted average SSTL, followed by UCHP and the honeycomb panel. From table 4, it could be seen that the U-shaped and V-shaped corrugation in the honeycomb core improved the unweighted average STL by approximately 19 dB and 25 dB respectively, showing a significant improvement in the noise attenuation properties.

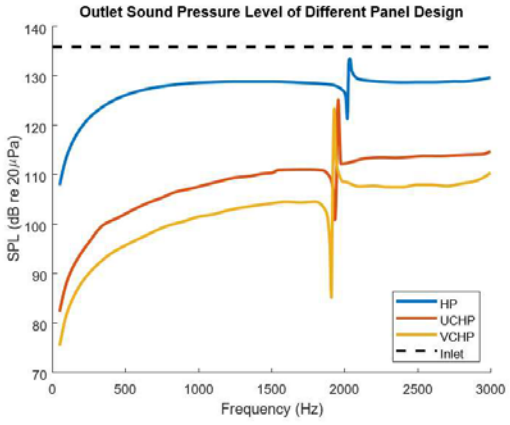

Figure 9. SPL_{out} of different panel design

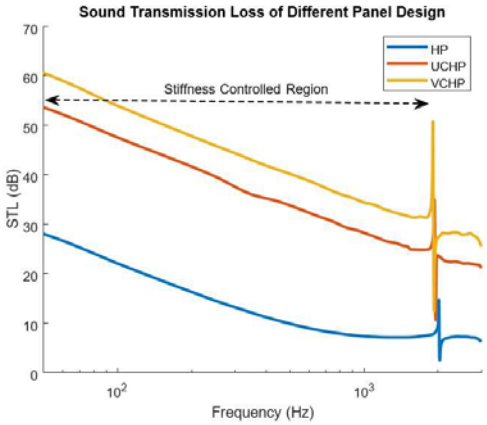

Figure 10. STL of different panel design

Table 4. Unweighted average STL (50-3000 Hz)

Panel	Unweighted Average STL (dB)
HP	8.54
UCHP	27.53
VCHP	33.58

3.3. Flow performance

Figure 11 illustrated the pressure distribution through the duct with different panel designs with an inlet flow velocity, u of $3\ \mathrm{m/s}$ and it could be seen that the pressure decreased when the flow approached the panel which was located from duct length, $L = 0.006$ m to $L = -0.006$ m as the air accelerated when passing through the perforated facings. The increase in fluid velocity when passing through the panel resulted in low pressure in the panel due to the conversion of energy as the fluid potential energy was converted into kinetic energy, The pressure was recovered at the downstream of the duct as the fluid decelerated and the excess kinetic energy was converted back into the pressure, causing the pressure to increase. From figure 11, more number of dips in pressure was also observed in UCHP and VCHP compared to the honeycomb panel as the flow experienced more contraction and expansion when flowing through the panels due to the presence of corrugated structure in the honeycomb core.

The pressure loss of different panel designs as a function of the inlet flow velocity, u was also shown in figure 12 and it could be observed that the pressure loss increased with inlet flow velocity for all the panel. It was also observed that the VCHP panel experienced the highest pressure loss, followed by the UCHP and the honeycomb panel. However, the difference between the pressure losses for the different panel design was relatively small and negligible, especially at low inlet velocity, when the open area was kept constant for all the panels. Hence, it could be concluded that the V-shaped and U-shaped corrugation in the honeycomb did not affect the flow performance of the honeycomb panel provided that the open area of the panel was kept constant.

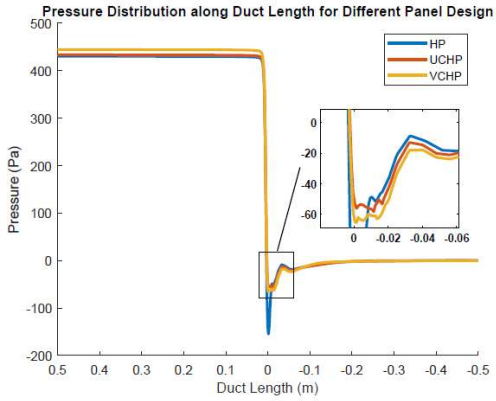

Figure 11. Pressure distribution along the duct at $u = 3.0\ \mathrm{m/s}$ for different panel design.

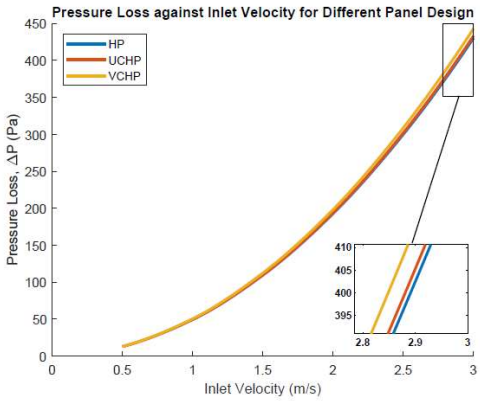

Figure 12. Pressure drop as a function of inlet velocity for different panel design.

4. Conclusion

A honeycomb sandwich panel with perforated facings was designed to allow the transfer of air and the numerical model had been developed for vibro-acoustic analysis and flow analysis. The honeycomb panel was improved through the use of corrugation structure in the honeycomb core and two different hybrid honeycomb designs (UCHP and VCHP) had been proposed. The UCHP and VCHP proposed consisted of U-shaped corrugation structure and V-shaped corrugation structure in the honeycomb core respectively. The unweighted STL of the UCHP and VCHP was found to be 19 dB and 25 dB higher than the honeycomb panel with minimal effect on the flow performance. With the improvement in the acoustic properties without significantly affecting the exchange of air, the proposed UCHP and VCHP design could allow the honeycomb panel to be used for wider applications which involved fluid flows such as in motors and compressors, especially when lightweight noise attenuating structure was required. As this paper only focused on the numerical study of the vibro-acoustic characterisation of the honeycomb panel with flow permeability, future work could be conducted to verify the acoustic as well as the flow properties of the panel through experiment verifications.

References

[1] Sui N, Yan X, Huang T Y, Xu J, Yuan F G and Jing Y 2015 *Appl. Phys. Lett.* **106** 171905
[2] Kim S H and Lee S H 2014 *AIP Adv.* **4** 117123
[3] Ma G, Yang M, Yang Z and Sheng P 2013 *Appl. Phys. Lett.* **103** 011903
[4] Huang H, Qiu X and Kang J 2011 *J. Acoust. Soc. Am.* **130** 176-88
[5] P`amies T, Romeu J, Genesc`a M and Arcos R 2014 *Appl. Acoust.* **84** 116-21
[6] Shen C, Xie Y, Cummer S and Jing Y 2017 *J. Acoust. Soc. Am.* **141** 3574
[7] Cho S J, Kim B S, Min D K, Cho Y S and Park J H 2016 *Compos. Struct.* **155** 1-7
[8] Han B, Wang W, Zhang Z, Zhang Q, Jin F, Lu T and Han B 2016 *Theor. App. Mech. Lett.* **6** 54-9
[9] Tang Y, Ren S, Meng H, Xin F, Huang L, Chen T, Zhang C and Lu T J 2017 *Sci. Rep.* **7** 43340
[10] Kim H S, Kim S R, Lee S H, Seo Y H and Ma P S 2016 *J. Acoust. Soc. Am.* **139** 2324
[11] Andersen K S 2008 *Proc. COMSOL Conf.*
[12] Howard C Q and Cazzolato B S 2015 *Acoustic Analysis Using MATLAB and ANSYS* (Boca Raton: CRC Press)
[13] Osipov A, Meesb P and Vermeif G 1997 *Appl. Acoust.* **52** 273-88
[14] Arunkumar M P, Pitchaimani J, Gangadharan K V and Babu M C L 2016 *Aerosp Sci Technol* **56** 155-67
[15] Smolenski C P and Krokosky E M 1973 *J. Acoust. Soc. Am.* **54** 1449-57
[16] Wang T, Li S, Rajaram S and Nutt S R 2010 *J. Vib. Acoust.* **132** 011004
[17] Brosig D, Mellert V and Remmers H 2010 Proc. *20th Int. Congress on Acoustics*